University of Huddersfield Repository

VanderMarel, Joel, Eadie, Donald T., Oldknow, Kevin D. and Iwnicki, Simon

A predictive model of energy savings from top of rail friction control

Original Citation

This version is available at http://eprints.hud.ac.uk/id/eprint/23217/

http://eprints.hud.ac.uk/

A PREDICTIVE MODEL OF ENERGY SAVINGS FROM TOP OF RAIL FRICTION CONTROL

Joel VanderMarel[1]*, Donald T. Eadie[1], Kevin D. Oldknow[1], and Simon Iwnicki[2]

1) LB Foster Friction Management, 4041 Remi Place, Burnaby, BC, V5A4J8, Canada

2) School of Computing and Engineering, University of Huddersfield, Queensgate, Huddersfield HD1 3DH, UK

*jvandermarel@lbfoster.com

ABSTRACT

In this paper the authors present a predictive model of train energy requirements due to the application of a top of rail friction modifier (TOR-FM) versus dry wheel / rail conditions. Using the VAMPIRE® Pro simulation package, train energy requirements are modeled for two sets of TOR-FM frictional conditions, one using full Kalker coefficients and the other by using a Kalker factor of 18%. Both scenarios use a top of rail saturated coefficient of friction of 0.35. Under both TOR-FM frictional conditions, train energy savings are shown for complete laps of the Transportation Technology Center Inc.'s (TTCI) Transit Test Track (TTT) loop, and also when isolating only the tangent section of the loop. However, the magnitude of energy savings varies greatly depending on the Kalker coefficient factor used, highlighting the need to model this relationship as accurately as possible. These simulation results are compared with data obtained from a field study, in which train energy savings of 5.3% (lap) and 7.8% (tangent) are shown due to the application of TOR-FM.

1 INTRODUCTION

1.1 Wheel / Rail Friction

Friction at the wheel / rail interface is understood to have significant impacts on wheel and rail wear, lateral (curving) forces, curve noise, and train energy (fuel usage) [1][2][3]. In recent years industry focus has been on the separate control of friction at (a) the gauge face / flange interface (traditional lubrication) and (b) the top of rail (TOR) / wheel tread interface. The latter requires special materials known as friction modifiers that provide (a) a controlled intermediate coefficient of friction (average $\mu = 0.35$ [4] as measured by a Salient Systems push tribometer) considered safe for braking and adhesion, and (b) a positive slope to the creepage / creep force curve beyond the point of creep saturation (referred to as positive friction) [5]. This paper describes modeling work aimed at better understanding the role and mechanisms of TOR friction control in reducing train energy requirements, and continues previous work presented in [6].

Friction between the wheel and rail should be considered as a function of creep (microslip). This relationship in turn is dependent on the properties of the interfacial layer between wheel and rail, the so-called Third Body [7]. The goal of friction control is to manipulate the composition of the Third Body to adjust the shear properties (yield strength) to achieve appropriate targets. Unfortunately, the subtleties of the creepage / creep force relationships under different frictional conditions are not well represented in current vehicle dynamics software packages.

1.2 Train Energy and Fuel Consumption

Locomotive fuel consumption and technologies to reduce train energy are major focus areas for heavy haul freight operators. There are a number of published reports of the impact of TOR friction control (TOR-FM) on fuel savings. Prior models have emphasized the

impacts of reduced curving resistance, predicting relatively low absolute energy savings in low curvature track, i.e. that the absolute fuel savings with TOR-FM is an exponential function of track curvature [3]. Recent work [8] has indicated that all three major data sets for heavily curved territory fall on the same exponential relationship. This suggests that in these territories the largest component of fuel savings with TOR-FM originates from reductions in curving resistance (lateral forces).

Other results have suggested that significant fuel savings are also achieved in areas of predominantly tangent track and shallow curvature [9]. These results deviate significantly from the relationship based on curve density described in [3] and [8]. As these territories represent the majority of the fuel consumption on heavy haul railways, it is important to provide a strong scientific underpinning to understanding and quantifying the effects of TOR-FM on train energy.

2 MECHANISMS FOR FUEL SAVINGS IN TANGENT / LOW CURVATURE TRACK

As noted above, one of the primary motivations for this work is the development of a practical understanding and modeling approach that allows for the prediction of energy savings in tangent and low curvature track due to friction control at the top of rail / wheel tread interface. In order to provide a working explanation for these results and the potential for an effective model, a hypothesis was formulated based on the potential influence of (a) inherent vehicle component misalignments and (b) persistent deviations from the neutral running position in tangent track. This study is part of an ongoing body of worked aimed at evaluating the validity and potential applicability of the hypothesis.

Vehicle component misalignments, e.g. angular misalignments between axles in bogie, are a practical reality in railroad operating conditions. The three-piece bogies that are typically used in North American

Heavy Haul freight are known to carry a potential for misalignment and / or slack in the mating of components in part due to the simplicity of the design (a strength from the standpoint of maintainability). The influence of this type of misalignment on energy spent at the wheel / rail interface was explored in [6].

The second component of the hypothesis is built around the potential for persistent deviations from the neutral running position in tangent track. After emerging from a curve, the final position and alignment of the bogie will be inherently variable due to (among other factors) the influence of sliding friction at the centerbowl. While steering forces will (assuming "good" wheel / rail profiles) act to provide a positive steering moment to center the bogie, there will be the possibility of an equilibrium between these positive steering forces and the counteracting forces arising from the centerbowl and other components. In the presence of a persistent (albeit small) angle of attack, there will be a resulting persistent creepage at the wheel / rail interface and corresponding energy dissipation. By reducing friction levels through top of rail friction control, the dissipation of energy through this mechanism may be reduced, contributing to an overall reduction in effective rolling resistance and energy spent in moving the train.

3 VERIFICATION OF PROPOSED TRAIN ENERGY MODEL / SAVINGS

In order to better understand the train energy requirements under different top of rail / wheel tread interface frictional conditions and develop a predictive model of these energy requirements, a two part approach is employed in this study. In the first, the VAMPIRE® Pro simulation package is used to develop the predictive model of train energy requirements using the Tγ method outlined in Section 5.1 and fully derived in [6]. The simulation parameters were chosen to match closely with train energy data made available from a field study undertaken at the Transportation Technology Center Inc.'s (TTCI)

Facility for Accelerated Service Testing (FAST). This field data is subsequent examined in the second part of the study. As such, for both parts of the study, the TTCI Transit Test Track (TTT) loop was utilized. The TTT loop consists of a 15 kilometer loop with a 2200 meter radius curve (with 50.8 mm cant), and two 1200 meter radius curves (both with 114.3 mm cant), and a 3 kilometer tangent track section with minimal grade as shown in Fig. 1. Train energy requirements were calculated for the entire loop and also for only the tangent section.
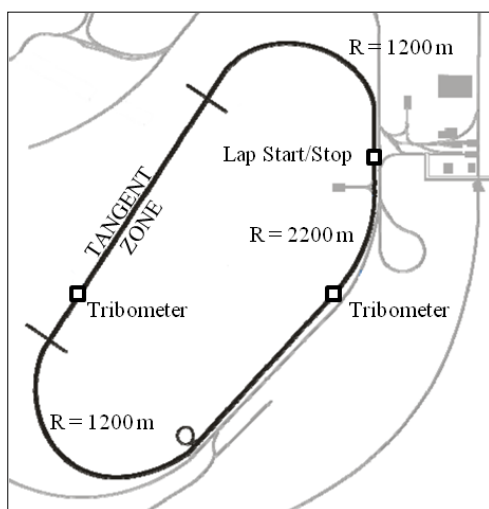

Fig. 1. TTCI Transit Test Track (TTT) loop showing track geometry and location of tribometer measurements used in field study

4 FIELD TESTING AT TTCI-TTT

4.1 Proposed Test Procedure

For the aforementioned field study, which was undertaken on the TTT loop to evaluate the effects of TOR friction control on train energy requirements, a train consisting of two SD 70-M locomotives and 29 loaded 138-tonne gross weight coal hopper cars was used. An empty hopper car equipped with an onboard TOR friction modifier application system was placed directly following the locomotives which provided an air atomized spray of KELTRACK® friction modifier to the TOR surface. The mechanical train energy requirement was measured by means of an instrumented coupler placed between the TOR-FM

system equipped car and the first loaded hopper car. Furthermore, Salient System push tribometers were used to measure TOR friction levels at two points in the loop, including upon entering the tangent section.

4.2 Analysis of TTCI Field Results

The following graph shows the mechanical energy calculated versus the average TOR COF for both the complete lap readings and the tangent section only.
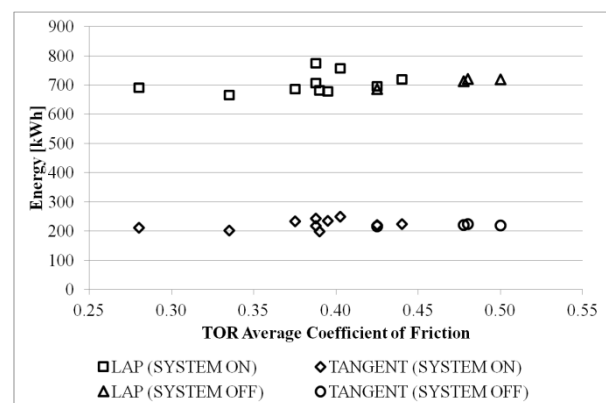

Fig. 2. Lap and tangent mechanical energy versus average TOR COF for nominal train speed of 22 m/s (50 mph).

During the initial test laps it was apparent, from both the tribometer and energy readings, that there was a poor transfer rate of friction modifier from the spray system to the top of rail surface. The primary reason was suspected to be high wind effects around the nozzle tip, causing only a portion of the total application rate of the atomized friction modifier to reach the rail. During subsequent laps, the nozzle wind skirt design was modified, resulting in better friction modifier deposition as shown by TOR coefficients of friction closer to those expected from previous tribometers measurements [4]. However, due to time constraints, this limited the number of valid laps for both the baseline dry and 'system on' to three for each condition set. The average energy requirements for both the complete lap and isolated tangent section are shown in Fig. 3 and Fig. 4 respectively.
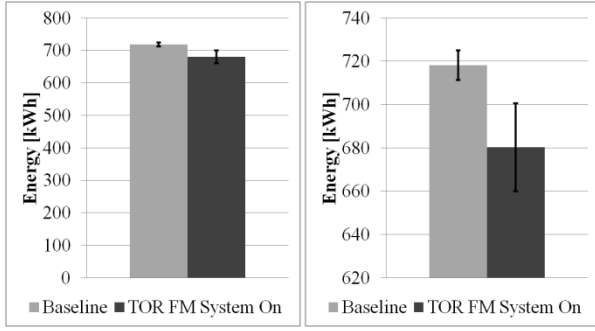
Fig. 3. Average mechanical energy requirements measured for entire TTT lap. Note graph on right is rescaled to show 90% confidence intervals. Nominal train speed of 22 m/s (50 mph).
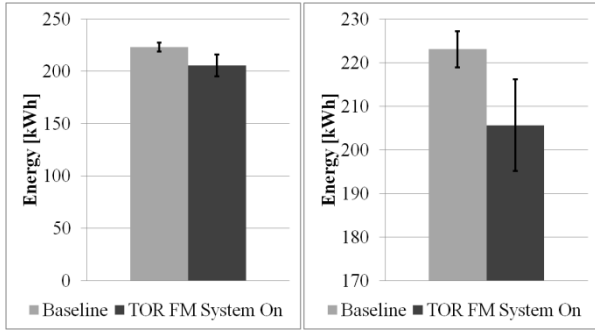

Fig. 4. Average mechanical energy requirements measured for TTT tangent section. Note graph on right is rescaled to show 90% confidence intervals. Nominal train speed of 22 m/s (50 mph).

The following table shows the percent change in energy requirements between the dry baseline and friction modified laps.

Table 1. Percent Change in Energy Due to TOR FM

	Average [kWh]	Std. Dev. [kWh]
Lap Baseline (Dry)	718.2	4.1
Lap TOR FM System On	680.3	12.4
Percent Change in Lap	**-5.3 %**	
Tangent Baseline (Dry)	223.0	2.5
Tangent TOR FM System On	205.6	6.4
Percent Change in Tangent	**-7.8%**	

Average energy requirements and standard deviations based on mechanical force required to pull 29 loaded 138-tonne gross weight hopper cars

5 PROPOSED TRAIN ENERGY MODEL

5.1 Energy Expended at the Contact Area

The predictive train energy model used in this study is based on an integral of power dissipated at the wheel / rail contact area. For each wheelset the energy expended at the contact patch is influenced by the forward speed of the train, and the subsequent creep forces which arise in the left, right and flange contact areas. Therefore, the incremental energy expended at the collective sum of a single rail car's contact areas (denoted as ∂W), over a forward vehicle displacement of ∂x can be calculated using the following equation:

$$\partial W = \sum_{i=1}^{n} (T\gamma_{TOT})_i \, \partial x \qquad (1)$$

Where n denotes the number of axles on the rail car and $T\gamma_{TOT}$ denotes the summation of the left, right and flange $T\gamma$ wear numbers [6].

5.2 Total Train Energy Requirements

The above model neglects to include the effects of bearing resistance and aerodynamics. To include these effects, the following formula is used, which defines the total resistive force acting on a train in motion:

$$R_{total} = R_{tangent} + R_{curves} + R_{grade} \qquad (2)$$

For the first term the Canadian National (CN) train resistance formula is used, the second is the additional resistance due to curves and the last term is the additional resistance due to grades. Note that since the TTT is a closed loop, the net sum of the energy expended due to grade effects equals zero and that additional resistance due to wind has been neglected. Substituting in the CN train resistance formula (converted to SI units) gives [10]:

$$R_{total} = 7.35 + \frac{80.1N}{W} + 0.33V + \frac{CaV^2}{W} + R_{curves} \qquad (3)$$

Where:

R$_{total}$ = total relative resistance force (N/tonne)

W = total car weight (tonne)

N = number of axles

V = vehicle speed (m/s)

C = Canadian National streamlining coefficient

a = Cross-sectional area of the car

The predominant contributors to the first, third and fifth term are rolling resistance, flange resistance and curve resistance respectively and are, at least in part, affected by the TOR coefficient of friction. The second and fourth terms are primarily affected by bearing resistance and aerodynamics respectively and are predominantly not influenced by the application of a TOR friction modifier. As such the total train resistance can be broken into terms affected by the TOR COF and those which are not.

$$R_{total} = R_{TOR\,COF} + R_{other} \qquad (4)$$

In order to compare the total train energy effects of dry versus TOR-FM conditions, and assuming the R$_{other}$ term remains constant between both condition sets, Equation (4) can be rewritten as:

$$\frac{R_{total}^{FM} - R_{total}^{dry}}{R_{total}^{dry}} = \frac{R_{TOR\,COF}^{FM} - R_{TOR\,COF}^{dry}}{R_{TOR\,COF}^{dry}} \left(\frac{R_{TOR\,COF}^{dry}}{R_{total}^{dry}} \right) \qquad (5)$$

Where superscripts denote either dry or TOR-FM wheel / rail frictional conditions.

6 MODELING OF TRAIN ENERGY REQUIREMENTS

6.1 Modeling of Friction Modifiers

The relationship between microslip or creepage and creep forces for two bodies in rolling / sliding contact is linear for low creepages, but as the tangential force approaches the coulomb friction limit the relationship becomes non-linear and the lateral, longitudinal and spin creepages affect each other. The well known

'Kalker coefficients' are often used to describe the linear relationships, and in VAMPIRE® these are evaluated using a pre-calculated table of creep coefficients based on Kalker's CONTACT program. The inputs to this table include the contact ellipse semi-axes as well as the creepages.

In reality the creepage / creep force relationship is affected by the prevailing friction characteristics in a more complex way and this is often accounted for by factoring the Kalker coefficients to provide a better match between simulation results and test data. The creep forces at saturation can also be affected by the level of creepage (e.g. positive friction characteristics) and this is not correctly modelled by CONTACT.

Suda et al. [11] produced a creepage / creep force curve for both dry and friction modified wheel / rail conditions (friction modifier identified as KELTRACK® HPF) using a two-roller rig set-up. Recently, Fries et al. [12] showed that this friction modified traction-creepage curve can be bounded by curves of 16 and 20% Kalker factors. Similarly as in their study, Kalker factors of 18% are subsequently used to model friction modifiers. Fig. 5 shows the original plots produced by Suda et al. [11] with normalized longitudinal traction / creepage data exported from the VAMPIRE® simulation runs during this study.
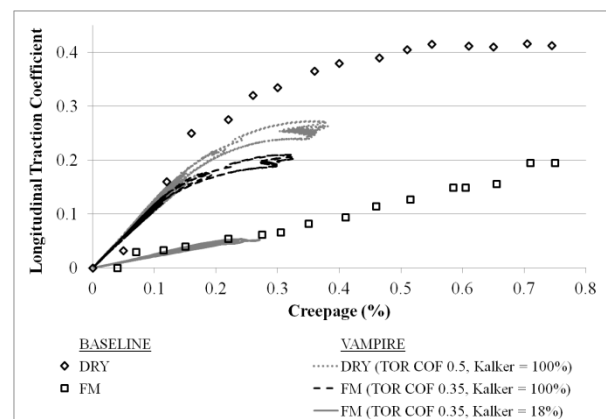

Fig. 5. Traction Creepage Curves for Dry and Friction Modified Wheel/Rail Condions. Baseline values from Suda et al. study [11].

The 100% Kalker simulation curves match well with the experimental data at low creepage values. The

deviation seen at higher creepages can be explained by the fact that the total tangential traction force must fall below the product of the coefficient of friction and the normal force given by the law of friction. As such, the experimental data comprises of a purely longitudinal creepage scenario, while the simulation data shows only the longitudinal component of a simulation containing longitudinal, lateral and spin creepages.

The 18% Kalker simulation data shows good agreement with the experimental data across the range of creepages experienced in the TTT simulations. It is apparent that simply lowering the saturated COF is inadequate to accurately simulate the effect of friction modifiers.

6.2 Modeling Parameters and Variables

Using the Tγ method, the energy expended at the contact patch was calculated using the VAMPIRE® Pro (5.60) simulation package and a complete model of a typical 130-tonne gross weight loaded coal car with three piece bogies. This model included individual coil spring elements to account for the outer, inner and control coil vertical non-linearities and spring group shear and torsional stiffnesses. Clearances between the sideframes and bearing adapters, bolster gib clearance and center plate radial gaps were also included. Two dimensional friction elements allow realistic modeling of the energy dissipation at the contact surfaces between the friction wedges and the side bearer and at the centre bowl. Due to the large number of non-linear elements, the simulations were run around the TTT loop four consecutive times, with results averaged from laps 2 through 4.

The vehicle was run over the Transit Test Track in two different scenarios. In the first, a full TTT loop including all track irregularities was used to provide comparable run data to the TTCI field study. In the second, the tangent section of the track was isolated (including all track irregularities) in order to examine the effect of the vehicle exiting the preceding curve had on the Tγ values. For this tangent only track, a 100

meter tangent section with no track irregularities was added to the front of the track file.

In order to investigate the effects of the application of a TOR friction modifier the following three TOR friction scenarios where employed:

1) Dry: TOR coefficient of friction is set to 0.5 [4] with a 100% Kalker factor.

2) Friction Modifier (corrected): TOR coefficient of friction set to 0.35 [4] with the Kalker coefficients modified by a factor of 18% [12].

3) Friction Modifier (uncorrected): TOR coefficient of friction set to 0.35 [4] with a 100% Kalker factor. This scenario represents the traditional method used to model friction modifiers.

All simulations were run at a speed of 22.4 m/s (50 mph). Also, frictional conditions at the flange / gauge corner were modeled as dry (COF = 0.5, Kalker = 100%).

Furthermore, for each frictional condition, six sets of wheel/rail contact profiles were tested.

1) New wide flange wheel profile with new 119 lb rail. Contact condition denoted as NEW 1 (WIDE FL.)

2) New narrow flange wheel profile with new 119 lb rail. Contact condition denoted as NEW 2 (NAR. FL.)

3) Four sets of worn profiles on worn 119 lb rail. Each worn wheel profile set consists of four pairs of individually measured left and right wheel profiles for each axle of the rail car. Each axle set was matched with a worn 119 lb rail profile taken on the tangent section of the TTT loop. These sets are labeled as WORN 1 through WORN 4 in subsequent sections.

7   SUMMARY OF MODELING RESULTS

7.1 Effect of Preceding Curves on Tangent Running

The following figures compare the lateral displacement and angle of attack of the leading wheelset for the rail

car model running over the isolated tangent section and running over the same section after having completed the first half of the TTT loop and exiting the 1200 meter radius curve. Fig. 6 and Fig. 7 show the results of dry TOR friction conditions. Fig. 8 and Fig. 9 are for TOR-FM friction conditions. Note all figures shown were modeled using the NEW 1 (WIDE FL.) wheel / rail contact data.
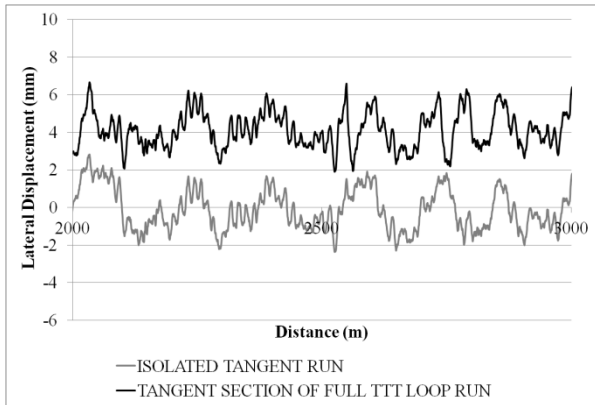

Fig. 6. Lateral displacement of leading wheelset for dry (TOR COF = 0.5, Kalker 100%) conditions. Note only portion of tangent section shown for clarity.
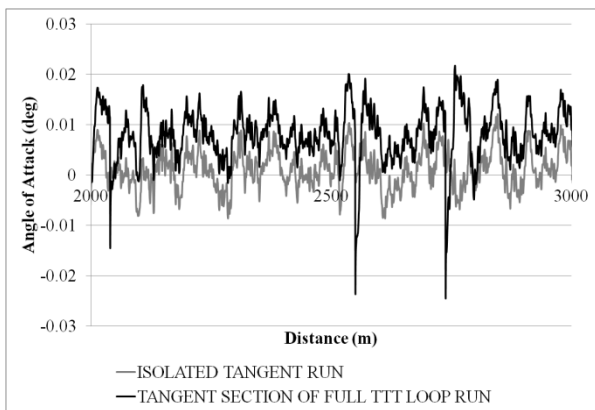
Fig. 7. Angle of attack of leading wheelset for dry (TOR COF = 0.5, Kalker 100%) conditions. Note only portion of tangent section shown for clarity.
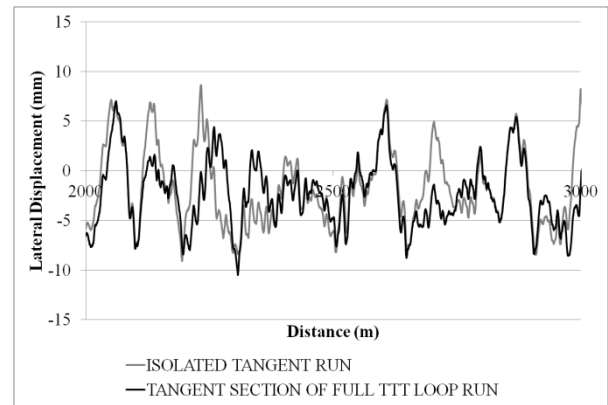

Fig. 8. . Lateral displacement of leading wheelset for TOR-FM (TOR COF = 0.35, Kalker 18%) conditions. Note only portion of tangent section shown for clarity.
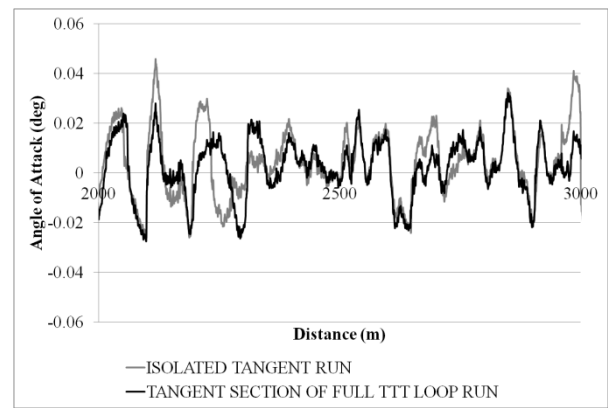

Fig. 9. Angle of attack of leading wheelset for TOR-FM (TOR COF = 0.35, Kalker 18%) conditions. Note only portion of tangent section shown for clarity.

As hypothesized, the above figures demonstrate the emergence of persistent lateral displacements and angles of attack after significant track perturbations (e.g. curves) under dry TOR frictional conditions. However, these persistent offsets are not apparent under the TOR-FM frictional conditions (using a Kalker factor of 18%), although the magnitude of the lateral displacements and angles of attack are larger than for the dry conditions. Similarly, these trends are continued in the Tγ summations as shown in Fig. 10 and Fig. 11.
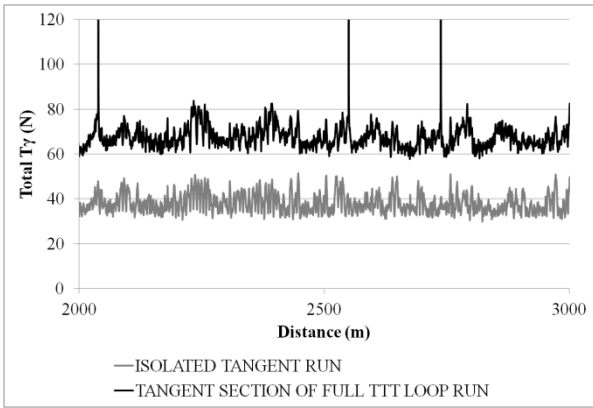
Fig. 10. Total Tγ sum for entire rail car for dry (TOR COF = 0.5, Kalker 100%) conditions. Note only portion of tangent section shown for clarity.
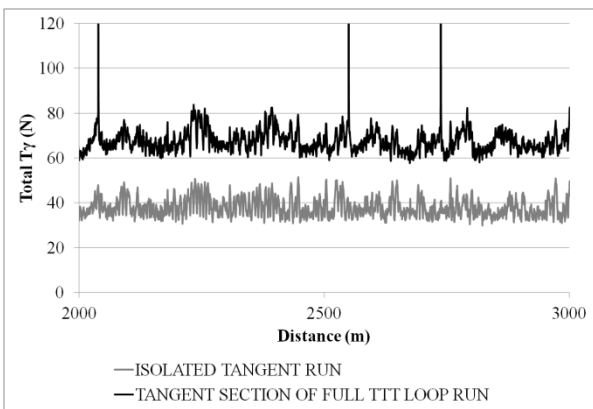

Fig. 11. Total Tγ sum for entire rail car for dry (TOR COF = 0.35, Kalker 18%) conditions. Note only portion of tangent section shown for clarity.

The persistent offset in the lateral displacements and angles of attack developed in the tangent running sections of the TTT loop under dry running conditions corresponds to an increase in energy expended at the contact patch and thus an increase in total train energy requirements.

7.2 Train Energy Requirements for Dry versus Friction Modifier Treated Rail

The following two figures show the percent change in energy requirements for both an entire TTT lap and only the tangent section due to using one of the two TOR friction modifier modeling scenarios versus dry wheel / rail contact. Energy requirements from the dry contact conditions simulations were used as the baseline values.
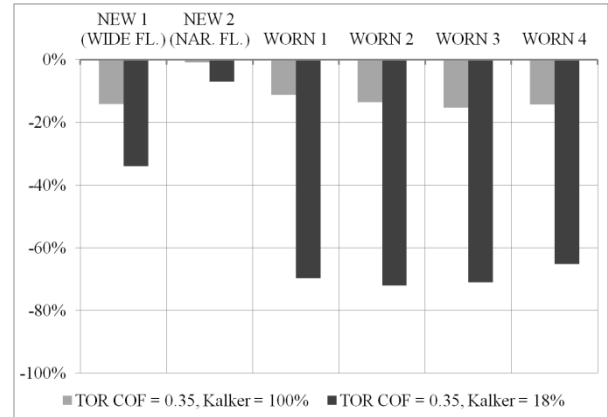

Fig. 12. Percent change in energy expended at the contact patch for an entire TTT lap from dry wheel / rail contact conditions. Energy requirements from dry frictional conditions used as baseline.
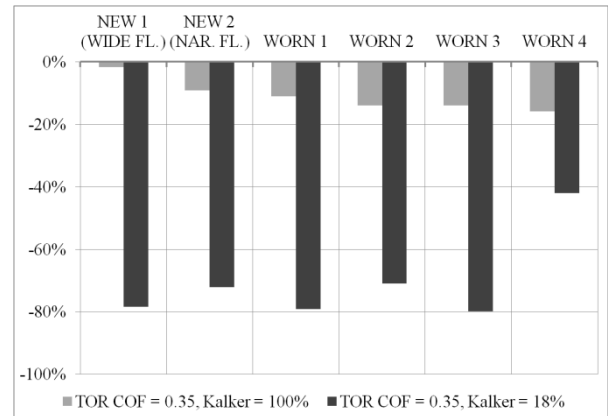

Fig. 13. Percent change in energy expended at the contact patch for tangent section of the TTT lap from dry wheel / rail contact conditions. Energy requirements from dry frictional conditions used as baseline.

Fig. 12 and Fig. 13 show reduced train energy requirements for both methods used to model TOR friction modifiers (i.e. with Kalker factors of 100% or 18% with a saturated COF of 0.35). Using full Kalker coefficients shows a reduction of train energy requirements of 1% to 15% for the entire lap and 2% to 16% for the tangent section of track. However, using a Kalker factor of 18% shows a reduction of train energy requirements of 7% to 72% for the entire lap and 42% to 80% for the tangent section of track.

Using Equation (5) and the percent changes in total train energy requirement seen in the field study, this suggests that by using a Kalker factor of 100%, the portion of total train energy affected by TOR-FM varies from 35% to 100% for the lap and 48% to 100%

in tangent running. Similarly, using a Kalker factor of 18% shows the portion of total train energy factors affected by TOR-FM varies from 7% to 76% for the lap and 10% to 19% in tangent running.

8   CONCLUSIONS

Using the VAMPIRE® Pro simulation package, the authors continue to develop a predictive model of train energy requirements under the influence of various top of rail frictional conditions. By using a Kalker factor of 18%, good agreement is shown between the simulation creepage / creep force curves and comparable curves obtained from experimental data. However, when correlating the changes in train energy requirements from the simulations with the field data, the results suggests that either the reduced Kalker coefficients over-exaggerate the obtainable reductions in train resistance or that the portion of total train energy resistances affected by TOR frictional conditions is quite small, especially in tangent running. Unfortunately only limited data exists for both of these key aspects, that is, field data of train energy requirements under comparable conditions for the use of TOR-FM versus dry conditions, and a complete set of creepage / creep force curves for friction modifiers under combined longitudinal, lateral and spin creepage conditions. As part of this ongoing research, it is the authors' intentions to continue pursuing a greater understanding of these two areas of knowledge.

REFERENCES

[1]   D. Eadie, B. Vidler, N. Hooper, T. Makowsky, Top of Rail Friction Control: Lateral Force and Rail Wear Reduction in a Freight Application, Proceedings of the International Heavy Haul Association, Fort Worth, Texas, May 2003.

[2]   D. Eadie, M. Santoro, J. Kalousek, Railway Noise and the Effect of Top of Rail Liquid Friction Modifiers: Changes in Sound and Vibration Spectral Distributions in Curves, Wear 258 (2005) 1148-1155.

[3]   J. Cotter, D. Eadie, D. Elvidge, N. Hooper, J. Roberts, T. Makowsky and Y. Liu, Top of Rail Friction Control: Reductions in Fuel and Greenhouse Gas Emissions, Proceedings of the International Heavy Haul Association, Fort Worth, Texas, May 2003 (7pp).

[4]   P. Sroba, M. Roney, R. Dashko, E. Magel, Canadian Pacific Railway's 100% Effective Lubrication Initiative, Proceedings AREMA Conference and Exhibition, Chicago, Illinois, 2001.

[5]   D. Eadie, J. Kalousek, K. Chiddick, The Role of High Positive Friction (HPF) Modifier in the Control of Short Pitch Corrugations and Related Phenomena, Wear 253 (2002) 185-192.

[6]   J. VanderMarel, S. Iwnicki, P. Klauser, K. Oldknow, D. Eadie, W. Kennedy, Energy Savings from Top of Rail Friction Control on Heavy Haul Freight Operations, Proceedings of the International Association of Vehicle System Dynamics Symposium, Manchester, UK, August 2011.

[7]   J. Kalousek, K. Hou, E. Magel, K. Chiddick, The Benefits of Friction Management – A Third Body Approach, Proceedings of the World Congress Conference of Railroad Research, Colorado Springs, June 1996, 461-467.

[8]   J. Cotter, D. Eadie, J. VanderMarel, K. Oldknow, S. Iwnicki, Impact of Top of Rail Friction Modifiers in Reducing Train Curving and Rolling

Resistance in Heavy Haul Applications, Proceedings of the International Heavy Haul Association, New Delhi, India, February 2013.

[9] R. Reiff, Mobile-based Car Mounted Top of Rail Friction Control Application Issues – Effectiveness and Deployment, TTCI Technology Digest TD-08-039, October 2008 (4pp).

[10] Manual for Railway Engineering, Chapter 16 Part 2, Train Performance, AREMA, Washington, D.C., 2011.

[11] Y. Suda, T. Iwasa, H. Komine, M. Tomeoka, H. Nakazawa, K. Matsumoto, T. Nakai, M. Tanimoto, Y. Kishimoto, Development of Onboard Friction Control, Wear 258 (2005) 1109-1114.

[12] R. Fries, C. Urban, N. Wilson, M. White, Modeling of Friction Modifier and Lubricant Characteristics for Rail Vehicle Simulations, Proceedings of the International Association of Vehicle System Dynamics Symposium, Manchester, UK, August 2011.